INSTITUTE OF PHYSICS PUBLISHING METROLOGIA
Metrologia **43** (2006) 53–59 doi:10.1088/0026-1394/43/1/008

Primary pressure standards based on dimensionally characterized piston/cylinder assemblies

J W Schmidt[1], **K Jain**[2], **A P Miiller**[1], **W J Bowers**[1] **and D A Olson**[1]

[1] National Institute of Standards and Technology, 100 Bureau Drive, Gaithersburg, MD 20899-8364, USA
[2] National Physical Laboratory, Dr K S Krishnan Road, New Delhi - 110012, India

Received 22 July 2005
Published 18 November 2005
Online at stacks.iop.org/Met/43/53

Abstract
NIST has characterized two large diameter (35.8 mm) piston/cylinder assemblies as primary pressure standards in the range 0.05 MPa to 1.0 MPa with uncertainties approaching the best mercury manometers. The realizations of the artefacts as primary standards are based on the dimensional characterization of the piston and cylinder, and models of the normal and shear forces on the base and flanks of the piston. We have studied two piston/cylinder assemblies, known at the National Institute of Standards and Technology (NIST) as PG 38 and PG 39, using these methods. The piston and cylinder of both assemblies were accurately dimensioned by Physikalisch Technische Bundesanstalt (PTB). All artefacts appeared to be round within ±30 nm and straight within ±100 nm over a substantial fraction of their heights. PG 39 was dimensioned a second time by PTB, three years after the initial measurement, and showed no significant change in dimensions or effective area. Comparisons of the effective area of PG 38 and PG 39 from dimensional measurements, against those obtained with calibration against the NIST ultrasonic interferometer manometer (UIM), are in agreement within the combined standard ($k = 1$) uncertainty of the dimensional measurements and the UIM. A cross-float comparison of PG 38 versus PG 39 also agreed with the dimensional characterization within their combined standard uncertainties and with the UIM calibrations. The expanded ($k = 2$) relative uncertainty of the effective area is about 6.0×10^{-6} for both assemblies.

1. Introduction

Finely honed piston/cylinder assemblies are used around the world to generate pressures with high accuracy in the range 0.1 MPa to 1000 MPa. This is done by adding or subtracting known weights on the piston/cylinder assembly, which is oriented vertically in the Earth's gravitational field. The pressure can be known as well as the combined uncertainty of the weights and of the effective area of the piston/cylinder assembly. Often the effective areas are determined through a calibration to another piston gauge or to a mercury manometer. In some cases the piston and cylinder are large enough and uniform enough so that uncertainties in effective area determined from dimensional measurements can rival the best manometers.

The Pressure and Vacuum Group at the National Institute of Standards and Technology (NIST) has acquired two piston/cylinder assemblies (known within NIST as PG 38 and PG 39) and has established a history of both of them going back 15 years [1]. The two gauges are in effect twins with relatively large diameters and can, as a result of calibrations of their effective area with a NIST ultrasonic interferometer manometer (UIM), be confidently used with relatively low uncertainties over the pressure range 0.05 MPa to 1 MPa. The 15-year history of these gauges indicates that there has not been any increase or decrease in their effective areas, A_{eff}, within the uncertainty of the measurements.

In addition, characterizations based on recent dimensional measurements from the Physikalisch Technische

Bundesanstalt (PTB) and on older dimensional measurements from NIST's Precision Engineering Division agree well with the values of A_{eff} obtained with the UIM during the course of several years.

Recently, the UIM has been physically moved to NIST's new Advanced Metrology Laboratory (AML), which is a state-of-the-art facility with enhanced vibration isolation, humidity control and ambient temperature regulation of ±0.1 K (for the UIM laboratory). PG 38 and PG 39 have served as check standards for the move and measurements of their effective areas with the UIM before and after the move were well within the combined standard ($k = 1$) uncertainties of the individual set of measurements.

2. Apparatus

2.1. The NIST dimensional capability

In 1989, dimensional measurements by NIST's Precision Engineering Division of absolute diameters of pistons and cylinders involved a two-step process. First gauge blocks were wrung together to build a stack with total length within 2 µm of the diameter of the piston. A precision comparator was used to compare the length of the stack to the diameter of the piston at several places along two longitudes. The length of the gauge-block stack was then measured with a laser interferometer.

If similar measurements (roundness, straightness and absolute diameters) were to be done now at NIST they would all be performed on the Precision Engineering Division's coordinate measuring machine (CMM), which has recently been moved to the new AML with ±0.01 K ambient temperature regulation for the CMM laboratory. This facility avoids the extra calibration step, i.e. the comparison to gauge blocks, and gives the coordinates of the surface points directly, to an accuracy of about 35 nm ($k = 1$) and would imply a relative uncertainty in an area of about two parts in 10^6. Dimensional characterization of PG 38 and PG 39 with the NIST CMM is being planned for the near future.

2.2. The PTB dimensional capability

The piston and cylinder absolute diameters measured at PTB used a state-of-the-art diameter and form comparator [2, 3] in which a calibrating laser interferometer is integral to the apparatus. In the first measurement of PG 39 in 1999, the straightness errors were measured with the same device as the diameters, and the roundness errors were measured with Talyrond 73 [4]. In the measurement of both PG 39 and PG 38 in 2003, the modified cylinder form measurement instrument MFU8-PTB was used for both the straightness errors and roundness errors [5, 6].

2.3. The piston/cylinder assemblies

PG 38 and PG 39 are twin piston/cylinder assemblies acquired from Ruska Instrument Corp.[3] in 1989. The pistons, although hollow (see figure 1), are each made from single castings of tungsten carbide and have proved to be highly stable with respect to temperature changes and to other stresses normally encountered in their operation. Their nominal diameters are approximately 35.8 mm with radial clearances between pistons and cylinders of about 600 nm.

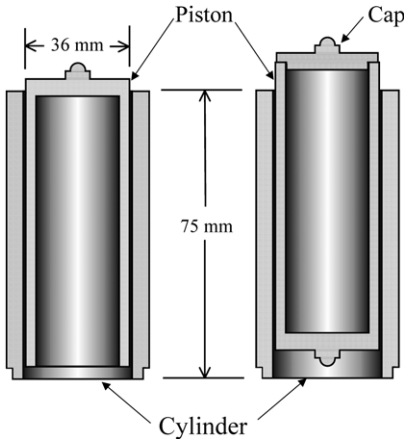

Figure 1. A schematic diagram of the PG 38 and PG 39 piston/cylinder assembly with the piston in upright (left) and inverted (right) orientations. The cap is used to support the weight carrier plus weights.

The construction of the pistons is such that they can be inserted into their cylinders either upright or inverted. When operated in the inverted configuration a special cap with a spherical pivot is placed onto the hollow end to allow masses to be loaded onto the inverted pistons. Although the inverted configuration might appear to be only a novelty as a pressure standard, it does allow simple formulae and models to be used in estimating the pressure coefficients of the assemblies. The inverted piston configuration has a different calculable value for the pressure coefficient than the upright configuration.

2.4. The ultrasonic interferometer manometer

The primary standard used at NIST to characterize piston gauges is a UIM with a full-scale range of 360 kPa. The unique feature of the UIMs developed at NIST [7–10] is that the change in height of the manometric-fluid surfaces (column heights) is determined by an ultrasonic technique. A transducer at the bottom of each liquid column generates a pulse of ultrasound (typically near 10 MHz) that propagates up the column, is reflected from the liquid–gas interface, and returns to be detected by the transducer. The change in phase of the returned signal is proportional to the length of the column (allowing for temperature and pressure corrections), and, with careful phase measurement, length changes of 10^{-5} mm can be detected. The manometers are otherwise conventional, although care has been taken to minimize error. For example they employ a W or three-column design to correct for possible tilt, large-diameter (75 mm) liquid surfaces to minimize capillary effects, thermal shields to stabilize the temperature and minimize its gradients, and high-vacuum techniques to minimize leaks and pressure gradients.

[3] In order to describe materials and experimental procedures adequately, it is occasionally necessary to identify commercial products by manufacturers' name or label. In no instance does such identification imply endorsement by the NIST, nor does it imply that the particular product or equipment is necessarily the best available for the purpose.

3. Measurements

The measurements of effective area, A_{eff}, consist of two types: (1) A_{eff} derived from dimensional measurements of the piston and cylinder diameters (traceable to the wavelength of an atomic transition in an HeNe laser interferometer) combined with models of the normal and shear forces on the base and flanks of the piston and (2) A_{eff} obtained from a calibration with NIST's UIM (traceable to the density of and speed-of-sound in mercury [7, 9]). In addition, through direct cross-float of PG 38 to PG 39, we have measured the ratio of effective areas of the two piston gauges.

3.1. Dimensional measurements and force models

Both PG 38 and PG 39 were first dimensioned in 1989 at NIST [11] with equipment described in section 2.1. All measurements were made in a room that was temperature controlled at $(20.00 \pm 0.05)\,^{\circ}\text{C}$. Within this band, temperatures were measured to $\pm 0.01\,^{\circ}\text{C}$ and were corrected to $20.00\,^{\circ}\text{C}$ using a nominal thermal expansion coefficient. The measured data were compiled by Jain *et al* [1] and they estimated the total relative standard ($k = 1$) uncertainty in effective area of about 10×10^{-6}.

About 10 years later in 1999 one of the gauges (PG 39) was sent to PTB and dimensioned by its state-of-the-art facility described briefly in section 2.2. These measurements on PG 39 [4], which were briefly summarized by Jain *et al* [12] in 2003, consist of a more extensive set of measurements than the ones performed by NIST in 1989. Absolute diameters were obtained at four places on the piston and at four places on the cylinder, with a standard uncertainty of 15 nm. Relative roundness (at 5 latitudes) and relative straightness measurements (along 8 longitudes) were acquired with a standard uncertainty of 5 nm and 25 nm. These measurements showed that both the piston and cylinder were round to within 30 nm, the piston was straight to within 100 nm over a substantial fraction of its height and the cylinder was straight to within experimental uncertainty. The changes in diameter over the height for the piston were larger than the standard uncertainty in the measurement.

In 2003 both PG 38 and PG 39 were sent to PTB and dimensioned (PG 39 for the second time at PTB) [5, 6]. This time, absolute diameters were obtained at 10 places on the piston and 10 places on the cylinders, with a standard uncertainty of 12.5 nm and 25 nm on the piston and cylinder, respectively. Relative roundness and relative straightness measurements were obtained again at 5 latitudes and 8 longitudes (now, however, with a standard uncertainty of 50 nm). Four of the absolute diameter measurements in 2003 were at the same longitudinal locations as in 1999. The relative difference in diameters at the four locations ranged from -0.1×10^{-6} to -0.8×10^{-6}. This small change in dimension gives us confidence in the uncertainties provided by PTB and further evidence of the stability of the artefacts.

The low uncertainty of dimensional measurement requires that we consider the appropriate model for converting those measurements into 'effective area' when the piston gauge is used for generating pressure. The model needs to account for all of the forces on the piston: external mass load, surface tension (zero for a gas pressure medium as in the present case) and the surface forces produced by the pressure fluid (normal force on the piston base, shear forces on the piston flanks and normal forces on the piston flanks). The conventional method of defining the effective area as the average of the piston and cylinder area would imply a relative standard uncertainty in A_0 of 1.0×10^{-6}, due only to the dimensional uncertainty. However, the 'direct averages' model is valid only for two limiting cases: (1) perfectly straight and round artefacts (and hence zero normal forces on the piston); or (2) a piston and cylinder whose straightness errors with height sum to zero, such that the zero-shear fluid boundary between them has no slope [13].

The dimensional data were used in several models of varying complexity to calculate forces on the piston, and from that the effective area at zero pressure, A_0, and its uncertainty. In the simplest model, we averaged the absolute diameters. In a second model, the piston and cylinder diameters were fixed at the absolute diameters at the 5 latitudes and assumed to vary linearly between those latitudes, and the viscous flow solution was used through the crevice to calculate pressure and the resultant normal and viscous forces. In a third model, the relative straightness measurements were added to provide profile between the 5 latitudes, and the viscous flow solution was again used in the crevice. In the most complex model, the data on roundness, straightness and absolute diameters of the piston and cylinder were reconstructed in the form of cylindrical 'bird cages' providing a longitudinal and latitudinal crevice variation, and the viscous flow solution was used in the crevice (bird cage/viscous model). This final model was also solved with the two-dimensional bird cage, but now with a simulated flow of gas that interpolated between molecular flow and viscous flow in the crevice between the piston and cylinder (bird cage/interpolated model). All flow solutions used nitrogen.

The resulting value for A_0 is an average of the maximum and minimum values from all of these results. We have calculated A_0 in this fashion for PG 39 using the 1999 and 2003 PTB data, and PG 38 using the 2003 PTB data. These values are listed in table 1. For all three cases, A_0 was largest for the bird cage/viscous model, and smallest for the bird cage/interpolated model in absolute mode (the relative difference was 5×10^{-6}). We note that the value given in table 1 for PG 39 in 1999 [12] used an average of the bird cage/viscous model and the bird cage/interpolated model in gauge mode [14]. Had we used the same basis as for the 2003 data, the relative difference in A_0 between 1999 and 2003 would have been 1.1×10^{-6}.

The history of values of A_0 for PG 38 and PG 39 derived from dimensional measurements at NIST and PTB and from calibration with the UIM is illustrated in figures 2(*a*) and (*b*), respectively.

Strictly, to be totally consistent when comparing the A_0 from the UIM (absolute mode) and A_0 from dimensional measurements (gauge mode) one should adjust one or the other to compensate for the fact that in gauge mode the piston/cylinder is under 1 bar of hydrostatic pressure, while the piston/cylinder is under vacuum in absolute mode. We have not applied this adjustment to the values in table 1 because it is an order of magnitude smaller than other possible

Table 1. The history for PG 38 and PG 39 of values of A_0, the effective area at 23 °C and zero pressure, and b, the pressure coefficient.

Year	A_0/mm^2	$b/10^{-12}$ Pa	Based on
PG38			
1989	1007.9510 ± 0.0101		NIST Dim [1]
1991	1007.9508 ± 0.005	5.7 ± 3.0	UIM
1997	1007.9498 ± 0.0028	7.3 ± 3.7	UIM
2002	1007.9502 ± 0.0028	7.5 ± 2.4	UIM
2003	1007.9497 ± 0.0030		PTB Dim [9]
2005	1007.9487 ± 0.0028	8.0 ± 2.4	UIM
PG39			
1989	1007.9525 ± 0.0101		NIST Dim [1, 12]
1991	1007.9521 ± 0.005	3.1 ± 3	UIM
1997	1007.9482 ± 0.0027	8.2 ± 3.6	UIM
1999	1007.9517 ± 0.0022		PTB Dim [8]
2002	1007.9490 ± 0.0028	4.9 ± 1.9	UIM
2003	1007.9484 ± 0.0030		PTB Dim [10]
2004	1007.9498 ± 0.0028	8.8 ± 1.4	UIM
2005	1007.9485 ± 0.0028	5.5 ± 2.7	UIM
	Estimate of b	8.97 ± 1.12	Mean of analytical & FEA

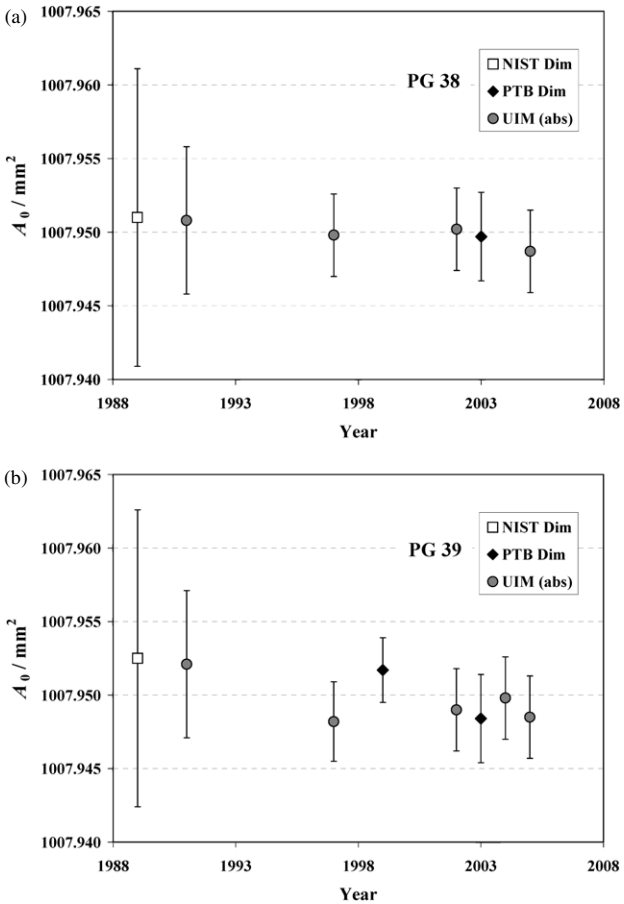

Figure 2. History of values for the effective area at 23 °C and at zero pressure for (*a*) PG 38 and (*b*) PG 39.

gas species and mode effects. We note that the difference is about

$$A_{\text{ambient}}(0)/A_{\text{vac}}(0) - 1 \sim -0.2 \times 10^{-6}.$$

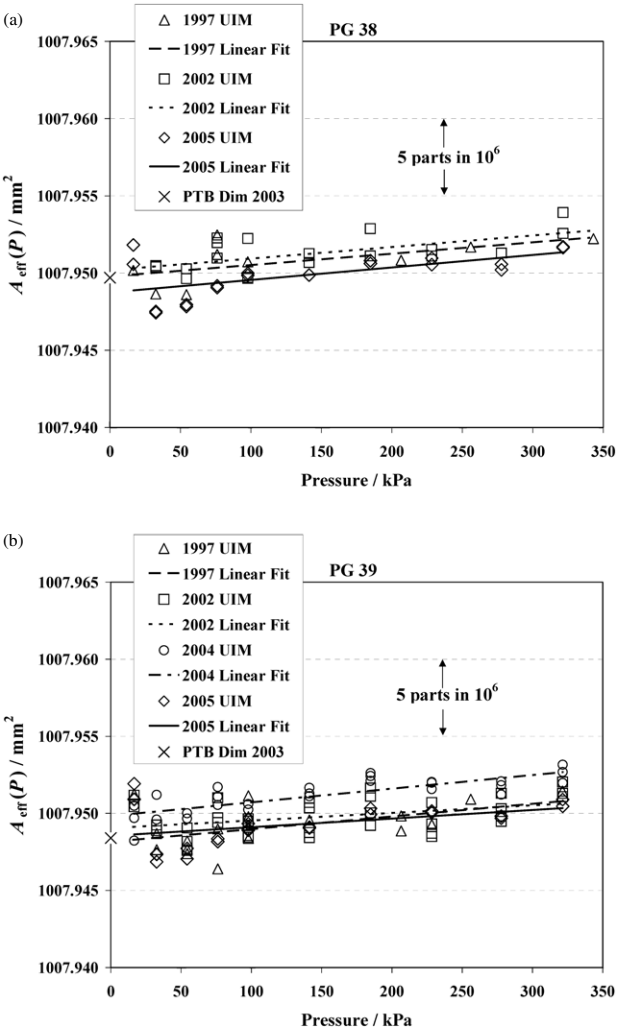

Figure 3. Effective area at 23 °C for (*a*) PG 38 and (*b*) PG 39 as measured by the UIM. The straight lines represent least-squares fits of linear functions of pressure to the individual sets of data.

3.2. Calibrations with the UIM

The effective area of each piston/cylinder assembly has been periodically calibrated with the UIM during the interval between 1991 and the present. Recent calibration results for the effective area at 23 °C of PG 38 and of PG 39, $A_{\text{eff}}(P)$, are plotted as a function of pressure in the nominal range 16 kPa to 322 kPa in figures 3(*a*) and (*b*), respectively. Linear functions of pressure were fitted to the individual sets of results using the least-squares method and these are illustrated as dotted, dashed and solid straight lines. Extrapolation of each linear function to zero pressure yields $A_0 = A_{\text{eff}}(0)$ as defined by

$$A_{\text{eff}}(P) = A_0(1 + bP). \tag{1}$$

The pressure coefficient b was calculated from the slope of each linear function. A history of values for A_0 and b that were obtained from calibrations with the UIM is given in table 1. All calibrations with the UIM were performed using nitrogen gas and with PG 38 and PG 39 in absolute mode, i.e. in a near vacuum.

3.3. The pressure coefficient

Because the uncertainties in A_0 have been substantially reduced from the earlier uncertainties, this now means that the uncertainties arising from the pressure coefficient have become comparable to the uncertainties in A_0 for piston gauges operating at higher pressures ($P > 1$ MPa). Consequently, more effort is being expended to reduce the uncertainties by understanding the pressure coefficients of the gauges[4].

With the goal of improving our knowledge of the pressure coefficient in mind, one of us (WJB) performed the cross-float measurements of PG 38 against PG 39 that exploited a design feature of the present gauges. That is the pistons can be operated in an inverted or closed end down orientation as well as the usual upright orientation (closed end up) as shown in figure 1. Because the pistons are hollow, that part of the gauge's pressure coefficient, b, due to the piston's distortion will be different in the inverted (down) orientation than in the usual orientation (up).

We can estimate with simple formulae from elasticity theory [17] the difference in b in the two orientations. Estimates give $b_{\mathrm{up}} \simeq 8.4 \times 10^{-12}$ Pa^{-1} and $b_{\mathrm{dn}} \simeq 1.2 \times 10^{-12}$ Pa^{-1}. The calculated difference in the pressure coefficients of the two configurations, $b_{\mathrm{up}} - b_{\mathrm{dn}}$, is thus about $\simeq 7.2 \times 10^{-12}$ Pa^{-1}. This difference can be readily measured if the piston gauges are cross-floated with one up and the other down.

Figure 4 shows the expected results (dashed lines) of four cross-floats plotted in the form of effective area ratios: $A_{38\,\mathrm{up}}(P)/A_{39\,\mathrm{up}}(P)$; $A_{38\,\mathrm{up}}(P)/A_{39\,\mathrm{dn}}(P)$; $A_{38\,\mathrm{dn}}(P)/A_{39\,\mathrm{dn}}(P)$; and $A_{38\,\mathrm{dn}}(P)/A_{39\,\mathrm{up}}(P)$. The expected results for the differences in pressure coefficients (slopes in figure 4) are

$$\Delta b_{\mathrm{up\text{–}up}} = 0.0 \times 10^{-12}\,\mathrm{Pa}^{-1},$$

$$\Delta b_{\mathrm{dn\text{–}dn}} = 0.0 \times 10^{-12}\,\mathrm{Pa}^{-1},$$

$$\Delta b_{\mathrm{dn\text{–}up}} = -7.2 \times 10^{-12}\,\mathrm{Pa}^{-1},$$

$$\Delta b_{\mathrm{up\text{–}dn}} = +7.2 \times 10^{-12}\,\mathrm{Pa}^{-1}.$$

These expectations are confirmed by the measurements obtained via cross-floats between the two gauges (open symbols):

$$b_{38\,\mathrm{up}} - b_{39\,\mathrm{up}} = (-1.07 \pm 0.78) \times 10^{-12}\,\mathrm{Pa}^{-1},$$

$$b_{38\,\mathrm{dn}} - b_{39\,\mathrm{dn}} = (-0.86 \pm 1.46) \times 10^{-12}\,\mathrm{Pa}^{-1},$$

$$b_{38\,\mathrm{dn}} - b_{39\,\mathrm{up}} = (-9.13 \pm 1.65) \times 10^{-12}\,\mathrm{Pa}^{-1},$$

$$b_{38\,\mathrm{up}} - b_{39\,\mathrm{dn}} = (+7.39 \pm 0.66) \times 10^{-12}\,\mathrm{Pa}^{-1}.$$

Figure 4 gives strong evidence that the model provided by elasticity theory is reasonably good, i.e. the largest difference between the measured Δb_{meas} and the calculated Δb_{calc} is 1.9×10^{-12} Pa^{-1}. Although we have assumed a rather simple pressure profile in the crevice, $P_{\mathrm{crevice}} = P/2$, the calculations for this design are not particularly sensitive to variations of crevice pressure. A difference in crevice pressure between 0 and full system pressure yielded an estimated change of b of only about $+0.92 \times 10^{-12}$ Pa^{-1}.

[4] The Atomic Pressure Standard (APS) is a project being developed at NIST that will offer an independent value for pressures in the 1 MPa to 7 MPa range [15, 16].

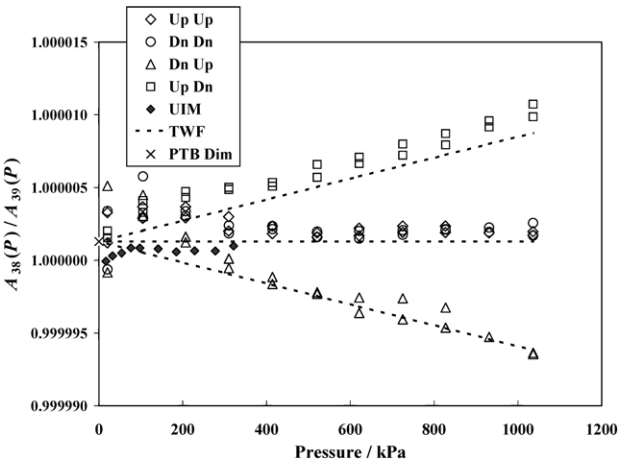

Figure 4. The ratio of effective area for PG 38 to that of PG 39. The open symbols indicate ratios from cross-floats of PG 38 versus PG 39 for different combinations of piston orientation. The solid diamonds indicate ratios from calibrations by the UIM. The dashed lines indicate ratios based on thick wall formulae from the elasticity theory. The symbol × represents the ratio based on dimensional measurements at PTB.

The simple formulae from elasticity theory neglect the constraint that the closed end makes on the pressure coefficient. Finite-element analysis (FEA) models can handle this constraint rather easily. A preliminary FEA model gave a slightly higher result for the pressure coefficient, $b_{\mathrm{up}} = 10 \times 10^{-12}$ Pa^{-1}.

For estimates of b_{up} and b_{dn} we have used a value for Young's modulus, $E = 6.0 \times 10^{11}$ Pa, and a literature value of Poisson's ratio, $\mu = 0.218$. The present values of Young's modulus were obtained from the time of flight of an ultrasonic pulse consisting of 100 cycles at 10 MHz [12]. In the future it will be possible to measure E and μ using resonant ultrasound spectroscopy (RUS), provided sample billets of the same material as the piston and cylinder can be obtained [18]. The RUS technique can provide both E and μ with high accuracy (relative standard uncertainties of 0.3%).

The ratios of effective area from the most recent calibrations of PG 38 and PG 39 (both upright) by the UIM are in good agreement with those based on the dimensional measurements as can be seen as the solid diamond symbols in figure 4. We note that the two bases used in the cross-float experiments are similar to each other but of a different design than the base used in the UIM calibrations. In particular the cross-float bases require that the pistons be floated with the top surface 5.5 mm above the top of the cylinder, while the UIM base allows the piston and cylinder surfaces to be flush during operation.

4. Estimates of uncertainty

The uncertainty in the effective area, $A_{\mathrm{eff}}(P)$, as given by equation (1), may be determined from uncertainties in the quantities A_0 and b, which are estimated using Type A and Type B evaluation methods described in [19, 20].

4.1. $u(A_0)$

The uncertainty in values of A_0 based on dimensional data arises from the uncertainty of the actual dimensional measurements and the uncertainty of converting these data to effective area when using various models for the forces acting on the piston. The standard uncertainties in the diameters given by the 2003 PTB data are $u(d) = 12.5$ nm and 25 nm for the piston and cylinder, respectively. Assuming the uncertainties in diameter are perfectly correlated between the piston and cylinder, this would imply a standard uncertainty in effective area of $u_{\mathrm{dim}}(A_0) = [u(d_{\mathrm{p}})/d_{\mathrm{p}} + u(d_{\mathrm{c}})/d_{\mathrm{c}}] \times A_0 \simeq 0.0011\ \mathrm{mm}^2$.

The uncertainty from all sources is estimated by considering the extremes of the effective area from various models, taking their mean, and assuming that the difference of the extreme from the mean is one standard deviation. The effective area has a relative difference of about 6×10^{-6} between the extremes. The standard uncertainty of the area from the models is thus $u_{\mathrm{flow}}(A_0) = 0.0030\ \mathrm{mm}^2$. The dimensional diameter uncertainty is included in the force models by increasing or decreasing all piston and cylinder diameters by their uncertainty. The uncertainty due to roundness and straightness is included by comparing the constructed diameters of the 'bird cage' model with the direct diameter measurements. Because the straightness and roundness traces cannot be fitted exactly together to build the 'bird cage', the construction necessarily contains strains at various points. The maximum strains tended to occur at the ends of the straightness traces. These were at most 50 nm, which is also the uncertainty of the straightness and roundness measurements. Various choices for resolving the strains resulted in changes in area of the order of $0.000\,14\ \mathrm{mm}^2$ for PG 38 and $0.000\,13\ \mathrm{mm}^2$ for PG 39. The largest variation in effective area occurred between the viscous flow model and the interpolated flow model.

The uncertainty in A_0 based on UIM measurements arises primarily from systematic effects in the UIM and from uncertainty in the masses that were used. The relative standard uncertainty due to the UIM is estimated to be 2.6×10^{-6} (5×10^{-6} in 1991) and that due to the masses is estimated as 1×10^{-6}. Combining these in quadrature, the total standard uncertainty in A_0 is estimated as $0.0028\ \mathrm{mm}^2$ ($0.005\ \mathrm{mm}^2$ for the 1991 value).

4.2. $u(b)$

To estimate the uncertainty in the pressure coefficient from elasticity theory we have started with a value calculated using simple analytical formulae, a measured value of Young's modulus and a literature value for Poisson's ratio [12]. In one instance the crevice pressure was modelled as half the system pressure. In other instances the crevice pressure was modelled at zero and then full system pressure, with the resulting change $\delta b = +0.92 \times 10^{-12}\ \mathrm{Pa}^{-1}$. In addition a preliminary FEA model was used with a result that was about $1.6 \times 10^{-12}\ \mathrm{Pa}^{-1}$ higher than the analytical model. (All these calculations are for the upright piston orientation.) Therefore the recommended value for b is the mean of the maximum ($10.0 \times 10^{-12}\ \mathrm{Pa}^{-1}$) and minimum ($7.95 \times 10^{-12}\ \mathrm{Pa}^{-1}$) values, i.e. $b = 8.97 \times 10^{-12}\ \mathrm{Pa}^{-1}$ with a standard uncertainty taken as $u(b) = (b_{\max} - b_{\min})/2$, which yields $1.03 \times 10^{-12}\ \mathrm{Pa}^{-1}$. When this is combined in quadrature with the uncertainty arising from Young's modulus (∼5%), the total standard uncertainty is

$$u_{\mathrm{tot}}(b) \simeq 1.12 \times 10^{-12}\ \mathrm{Pa}^{-1}.$$

The uncertainty in the values of b obtained from UIM measurements (see table 1) was calculated using the standard error in the slope of the linear fit to each set of data. The pressure coefficients determined from the mean of maximum and minimum values over the past UIM calibrations of PG 38 and PG 39 is $(6.9 \pm 1.2) \times 10^{-12}\ \mathrm{Pa}^{-1}$ and $(6.0 \pm 2.9) \times 10^{-12}\ \mathrm{Pa}^{-1}$, respectively, where the standard uncertainty is obtained from one-half the difference between maximum and minimum values.

4.3. $u[A_{\mathrm{eff}}(P)]$

The total relative standard uncertainty in the effective area for the gauges as a function of pressure based on the dimensional measurements and estimates of the pressure coefficient is

$$u(A_{\mathrm{eff}})/A_{\mathrm{eff}} = [(3.0 \times 10^{-6})^2 + (1.12 \times 10^{-12} P/\mathrm{Pa})^2]^{1/2}.$$

The total relative standard uncertainty in the effective area for the gauges as a function of pressure based on values of A_0 and b from calibrations by the UIM is:

PG 38: $u(A_{\mathrm{eff}})/A_{\mathrm{eff}}$
$= [(2.8 \times 10^{-6})^2 + (1.2 \times 10^{-12} P/\mathrm{Pa})^2]^{1/2}$,

PG 39: $u(A_{\mathrm{eff}})/A_{\mathrm{eff}}$
$= [(2.8 \times 10^{-6})^2 + (2.9 \times 10^{-12} P/\mathrm{Pa})^2]^{1/2}$.

5. Discussion

The small offset apparent in figure 4 of the cross-float results from the ratios based on UIM and dimensional measurements could be caused by a number of factors. First, two separate bases and two separate mass sets were used for the cross-float measurements, and another base was used for the UIM measurements. A systematic relative difference of 1.5×10^{-6} in the mass sets or possibly an unknown effect in the two bases used in the cross floats could cause the observed shift. In addition, in the cross-floats the top of the piston is 5.5 mm above the top of the cylinder, while for the UIM calibration the piston and cylinder tops are flush. Another possibility is that the cross-floats in gauge mode are subject to aerodynamic effects. On the other hand, a single base and a single set of masses were used for successive calibrations of PG 38 and PG 39 by the UIM and thus any base-related or mass-related systematic effects would disappear in their ratio. Furthermore the data from the UIM were taken in absolute mode and thus were not subject to aerodynamic effects.

6. Summary

NIST's Pressure and Vacuum Group has characterized two large diameter piston gauges via their dimensions and via a NIST UIM. The effective areas at $P = 0$ of the two characterizations agree well within the combined standard uncertainties of the two sources. The dimensions are based on

measurements from PTB's facility at Braunschweig, Germany. The calibrations are based on values obtained from the Pressure and Vacuum Group's 360 kPa UIM.

The pressure coefficients, b, were evaluated in three ways: (1) via estimates based on elasticity theory, (2) via cross-floats between the piston gauges in the up and down orientations and (3) via a calibration with the UIM. The pressure coefficient estimated from elasticity theory is $(8.97 \pm 1.12) \times 10^{-12}\,\mathrm{Pa}^{-1}$ and is an average of maximum and minimum values obtained using various models for forces on the flanks of the piston. The uncertainty assigned is half the difference in maximum and minimum values. With the cross-float experiments, the measured difference Δb between various combinations of piston orientation agrees with the calculated Δb to within a maximum difference of $1.9 \times 10^{-12}\,\mathrm{Pa}^{-1}$. The pressure coefficients determined from past UIM calibrations are $(6.9 \pm 1.2) \times 10^{-12}\,\mathrm{Pa}^{-1}$ and $(6.0 \pm 2.9) \times 10^{-12}\,\mathrm{Pa}^{-1}$ for PG 38 and PG 39, respectively.

The effective area from dimensions and from the UIM also agree at the maximum pressure of the UIM calibration (322 kPa) to within the standard uncertainty. The relative standard uncertainty in the effective area obtained from dimensional measurements plus force models extrapolated to 1 MPa yields about 3.2×10^{-6} for both PG 38 and PG 39. Here we have combined the uncertainties from A_0 and b in quadrature.

Based on the dimensional characterization, when used in calibrating secondary gauges in gauge mode, we recommend a value for the effective area of PG 38 at 23°C:

$$A_{\mathrm{eff}}(P) = 1007.9497\,\mathrm{mm}^2 \times (1 + 8.97 \times 10^{-12} P/\mathrm{Pa})$$

and for PG 39 we recommend

$$A_{\mathrm{eff}}(P) = 1007.9484\,\mathrm{mm}^2 \times (1 + 8.97 \times 10^{-12} P/\mathrm{Pa})$$

with standard uncertainties given by the following expression

$$u(A_{\mathrm{eff}})/A_{\mathrm{eff}} = [(3.0 \times 10^{-6})^2 + (1.12 \times 10^{-12} P/\mathrm{Pa})^2]^{1/2}.$$

Acknowledgments

The authors are very grateful to C R Tilford for providing data that he and one of us (KJ) obtained in calibrating PG 38 and PG 39 with the UIM in 1991 and 1997.

References

[1] Jain K, Ehrlich C, Houck J and Sharma J K N 1993 *Meas. Sci. Technol.* **4** 249–57
[2] Neugebauer M and Ludicke F 1998 *Proc. ASPE 1998 Annual Meeting (St Louis, MO)*
[3] Neugebauer M, Ludicke F, Bastam D, Bosse H, Reimann H and Topperwien C 1997 *Meas. Sci. Technol.* **8** 849–56
[4] PTB 1999 *Report* 5.31-99.148-3829
[5] PTB 2003 *Report* 5.31-03.4006607-4591/4592
[6] PTB 2003 *Report* 5.31-03.4006607-4593/4594
[7] Heydemann P L, Tilford C R and Hyland R W 1977 *J. Vac. Sci. Technol.* **14** 597–605
[8] Tilford C R 1977 *Appl. Opt.* **16** 1857–60
[9] Tilford C R 1987 *Metrologia* **24** 121–31
[10] Tilford C R and Hyland R W 1988 *Proc. XI IMEKO World Congress (Houston, TX)*
[11] Veale R C 1989 Precision Engineering Division—NBS *Report of Calibration* M3565
[12] Jain K, Bowers W and Schmidt J 2003 *J. Res. Natl Inst. Stand. Technol.* **108** 135–45
[13] Dadson R S, Lewis S L and Peggs G N 1982 *The Pressure Balance—Theory and Practice* (London: Her Majesty's Stationery Office)
[14] Schmidt J W, Tison S A and Ehrlich E D 1999 *Metrologia* **36** 565–70
[15] Moldover M R 1998 *J. Res. Natl Inst. Stand. Technol.* **103** 167
[16] May E F, Pitre L, Mehl J B, Moldover M R and Schmidt J W 2004 *Rev. Sci. Instrum.* **75** 3307
[17] Westergaard H M 1952 *Theory of Elasticity and Plasticity* (Cambridge, MA: Harvard University Press) chapter V
[18] Migliori A and Sarrao J 1997 *Resonant Ultrasound Spectroscopy* (New York: Wiley)
[19] 1993 *Guide to the Expression of Uncertainty in Measurement* (Geneva: International Organization for Standardization)
[20] Taylor B N and Kuyatt C E 1994 *Guidelines for Evaluating and Expressing the Uncertainty of NIST Measurement Results* NIST Technical Note 1297 (Washington, DC: US Government Printing Office)